Dynamics of Phasons; Phase Defects Formed on Dimer Rows, and Related Structural Changes of the Si(100) Surface at 80 K Studied by Scanning Tunneling Microscopy

Hidemi SHIGEKAWA*, Koji MIYAKE, Masahiko ISHIDA and Kenji HATA

*Institute of Materials Science, and Center for TARA, Tsukuba Advanced Research Alliance,
University of Tsukuba, Tsukuba 305, Japan*

Type-P defects, which are mobile phase defects on dimer rows with a structure similar to that of the type-C defect, were observed on Si(100) surface at 80 K, however, the observed surface structure was mainly $c(4 \times 2)$, contrary to the previous results obtained at 6 K. Complete $p(2 \times 2)$ arrangement was unstable, and type-P defects tended to form pairs with other type-P defects on neighboring dimer rows, resulting in a reduction of the area with complete $p(2 \times 2)$ arrangement. This is the first observation of the interacting phasons; type-P defects formed on Si(100) surface. The observed results were analyzed with the Ising model, and domain boundaries between $c(4 \times 2)$ and $p(2 \times 2)$ arrangements were found to play an important role in the dynamics of type-P defects at 80 K.

On many semiconductor (100) surfaces, pairs of top-layer atoms form dimers. Since these dimers comprise the basic reconstruction features of the (100) surfaces, and induce various interesting phenomena, the characteristics of dimer dynamics have been studied intensively. In the case of Si(100) surfaces, as Hamers *et al.* showed using scanning tunneling microscopy (STM),[1] dimers give rise to the observed (2×1) structure, and the asymmetric $c(4 \times 2)$ arrangement of buckled dimers has been accepted as the most stable phase.[2-6] However, details of the dynamics of dimer flip-flop motion and the interaction between buckled dimers have not yet been clarified and have attracted attention recently.[7-10]

Recently, changes in the buckled dimers and related structural changes on Si(100) surfaces were directly observed by STM at 6 K.[11] At 6 K, apparently symmetric dimers on a Si(100) surface, previously observed at 120–140 K, were almost frozen, and atomically resolved structural changes between the $c(4 \times 2)$ and $p(2 \times 2)$ arrangements of the Si(100) surface were observed. The observed changes were due to the fluctuation of a new type of phase defect, the type-P defect, on dimer rows. Since the type-P defect has a structure similar to that of the type-C defect, and acts as a phase shifter, migration of a type-P defect as a phason caused by the dimer flip-flop motion at the phase boundaries on dimer rows induces the apparent phase transition between the $c(4 \times 2)$ and $p(2 \times 2)$ arrangements. Also, at 6 K, a type-P defect on a dimer row seems to move almost independently of the arrangement of the dimer row with respect to the two adjacent dimer rows, which results in the formation of the observed $p(2 \times 2)$ arrangement in a large area.

In order to clarify the characteristics of the dimer flip-flop motion and the stability of the $c(4 \times 2)$ structure on a Si(100) surface, it is necessary to analyze the dimer features on an atomic scale at temperatures between 6 K and 120 K. In this work, we present the results of STM observation of the dynamics of dimer flip-flop motion on a Si(100) surface at 80 K.

A boron-doped ($\sim 0.01\,\Omega \cdot$ cm) Si(100) surface was heated to $\sim 1200°$C after prebaking for one day, and cooled to ~ 80 K. The base pressure was 1.0×10^{-8} Pa, and the pressure during heat treatment was kept below 5×10^{-8} Pa.

Figure 1 shows STM images taken during continuous scans at ~ 80 K. The surface was scanned in the constant current mode from left to right and top to bottom. Corresponding areas in the two images show the change taking place during a scan of about one minute. The sample voltage V_s and tunneling current It were set at $V_s = -2$ V and $I_t = 0.2$ nA. As shown in the figure, most of the observed surface was in the $c(4 \times 2)$ arrangement, and apparently symmetric dimers are formed at some boundaries between two mismatched phases. These phenomena are similar to those observed in previous STM experiments carried out at 120–140 K.[4,5,9] However, the surface was found to be more dynamic; changes in the buckling direction at phase boundaries on dimer rows induced fluctuation of the phase boundaries, i.e., type-P defects. Interaction between type-P defects on adjacent dimer rows was observed for the first time.

As indicated by the circles in Fig. 1(a), some phase defects were observed, which consisted of two defects similar to type-C defects, on adjacent dimer rows. They moved during one scan from P_1 and P_2 in Fig. 1(a) to P_1' and P_2' in Fig. 1(b). Therefore, the defects resembling a pair of type-C defects observed here are also phase boundaries formed by two type-P defects. The observed results indicate that there is some interaction between type-P defects.

Figure 2 shows magnifications of the images in Fig. 1. A single and a pair of type-P defects which moved during the scan are represented by red dots, while, those which remained in the same positions are represented by yellow dots. Some of the latter may be type-C defects. As seen in Fig. 2, type-P defects interact with each other; pairing and decoupling, and creation and annihilation of type-P defects were observed.

For example, the two type-P defects P_1 and P_2 in Fig. 2(a) formed the pair P_p during the scan. Magnifications of the areas shown in Figs. 2(a) and 2(b) are shown in Figs. 2(c) and 2(d), respectively; dimer arrangements around the type-P defects are indicated by dots. The buckling angle of dimers changes when a type-P de-
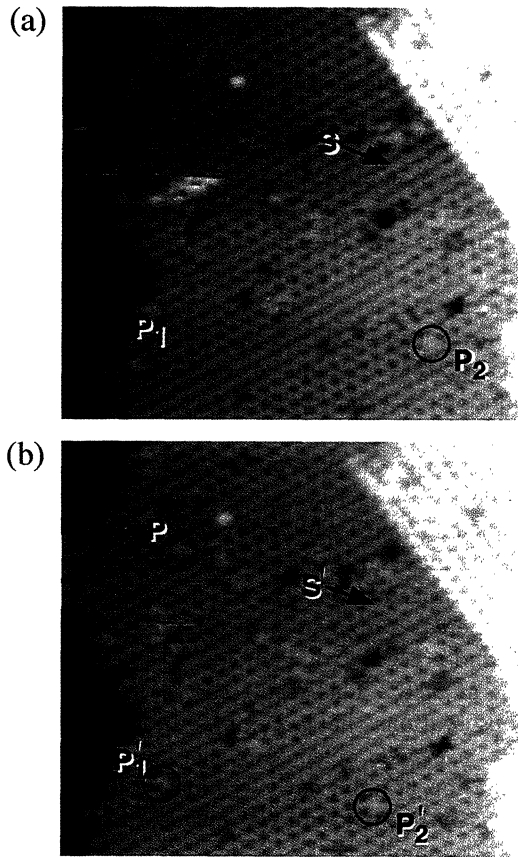
(a)

(b)

Fig. 1.   STM images of Si(100) surface obtained during continu-
ous scanning at ~80 K ($V_s = -2$ V, $I_s = 1.5$ nA).

(a)

(b)

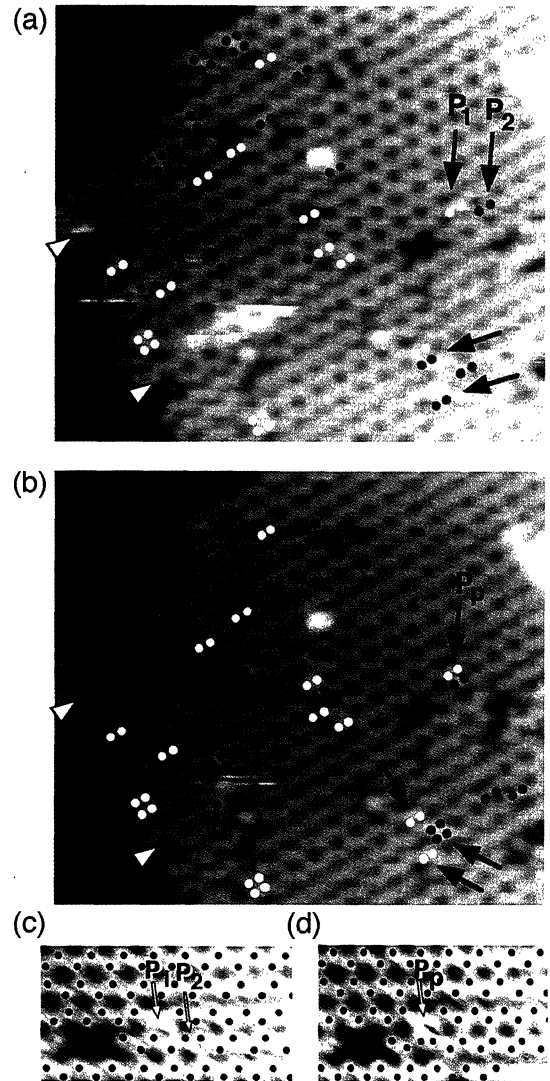(c)   (d)

Fig. 2.   (a), (b): Magnified images of the areas shown in Figs. 1(a)
and 1(b). One single and a pair of type-P defects, which change
position, are represented by red dots. Those which remained
in the same positions are represented by yellow dots. (c) (d)
Magnifications of (a) and (b) around P_1, P_2 and P_p. The white
bars indicate apparently symmetric dimers.

fect moves. Therefore, by comparing the dimer arrange-
ments in Figs. 2(c) and 2(d), it is clear that P_2 moved
towards the left by two dimer units and coupled with
P_1 to form the pair P_p: two dimers changed their buck-
ling angles. The pair of type-P defects was stable and
fluctuated along dimer rows as a single unit, as shown
in Fig. 1. However, when type-P defect pairs encounter
other type-P defects, they may recombine. One example
is indicated by the blue arrows in Fig. 2; the two pairs
of type-P defects in Fig. 2(a) interact with each other,
resulting in the formation of two single and one pair of
type-P defects, as shown in Fig. 2(b).

In spite of the dynamic changes in the dimers on an
atomic scale, the surface appears to be stable due to the
fact that the $c(4 \times 2)$ arrangement remained on the sur-
face, and complete $p(2 \times 2)$ domains were not formed
at 80 K. Apparently symmetric dimer domains, similar
to those observed by Wolkow *et al.* at higher tempera-
tures,[3-5] were observed as shown in Fig. 1. However,
these fluctuated back to form the $c(4 \times 2)$ arrangement
at 80 K. An example is shown in Fig. 1, as indicated by
S (Fig. 1(a)) to S' (Fig. 1(b)). No large $p(2 \times 2)$ domain
was formed, even in such fluctuation, which confirms the
fact that the $p(2 \times 2)$ arrangement is unstable at 80 K.

We consider the dynamics of the type-P defects and
the stability of the $c(4 \times 2)$ structure using the Ising
model.[10] Figure 3 shows schematic diagrams of the ar-
rangement of asymmetric dimers represented by Ising
spins. In general, the tilt angle of the buckled dimers
is assumed to take only two values, θ_0 and $-\theta_0$. There-

(a)   (d)
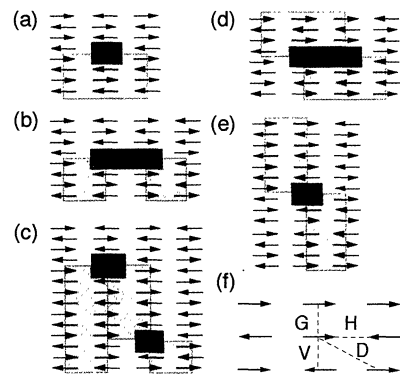
(b)   (e)

(c)

(f)

Fig. 3.   Schematics of $c(4 \times 2)$ dimer structures including type-P
defects: (a) a single type-P defect, (b) a pair of type-P defects,
(c) two single type-P defects, (d) a pair of type-P defects in
which four dimers are buckled in the same direction, (e) a single
type-P defect at the boundary between areas with $c(4 \times 2)$ and
$p(2 \times 2)$ structures. (f) The coupling constants defined in terms
of V, G, H, and D.

L 296   Jpn. J. Appl. Phys. Vol. 36 (1997) Pt. 2, No. 3A

H. Shigekawa et al.

fore, thermal motion of the dimers induces flip-flop motion between the two angles. The absolute values of the coupling constants (Fig. 3(f)) determined by Inoue et al. are $V = 51.9\,\mathrm{meV}$, $H = 6.6\,\mathrm{meV}$, and $D = 3.6\,\mathrm{meV}$. When a type-P defect exists, a structure with parallel spin is introduced. In this case the coupling constant V is modified and becomes G, about $40\,\mathrm{meV}$.

Figures 3(a) to 3(e) show schematics of dimer structures including type-P defects: (a) a single type-P defect, (b) a pair of type-P defects formed by two type-P defects on adjacent dimer rows, (c) two single type-P defects on adjacent dimer rows, (d) another type of a pair of type-P defects in which four dimers are buckled in the same direction, (e) a single type-P defect on a dimer row at the boundary between areas with $c(4 \times 2)$ and $p(2 \times 2)$ arrangements. Type-P defect units and areas with the $p(2 \times 2)$ arrangement, are indicated by red and gray rectangles in Fig. 3. Since two dimers have the same buckling angle in a type-P defect, the interaction energy E_{int} of a type-P defect is $-2V + G$, i.e., the observed fluctuation of type-P defects corresponds to the fluctuation of isolated high-energy phase defect regions.

Since the $p(2 \times 2)$ structure has a higher energy than that of the $c(4 \times 2)$ structure, a type-P defect is expected to move in order to reduce the size of a domain with $p(2 \times 2)$ arrangement shown in Fig. 3(b). Considering the properties of a type-P defect, the upper and lower dimers in a type-P defect unit shown in Fig. 3(a) have $c(4 \times 2)$ and $p(2 \times 2)$ arrangements with respect to the two adjacent dimer rows, and have interaction energies, E_{int}, of $-V + G + 2H - 4D$ and $-V + G - 2H + 4D$, respectively. Therefore, the lower dimer in the $p(2 \times 2)$ arrangement is less stable and tends to cause flip-flop motion, which also results in movement of the type-P defect towards the $p(2 \times 2)$ area and a reduction in the area with $p(2 \times 2)$ arrangement.

On the other hand, when two type-P defects form a pair as shown in Fig. 3(b), a dimer row which has complete $p(2 \times 2)$ arrangement with respect to its two adjacent dimer rows disappears, and four dimer rows become boundaries between areas with $c(4 \times 2)$ and $p(2 \times 2)$ arrangement, as shown in Fig. 3(b). A type-P defect pair has an interaction energy E_{int} of $-4V + 2G + 2H - 2D$, which is higher than that of two isolated type-P defects by $2H - 2D$. However, dimers on the phase boundaries have an interaction energy E_{int} of $-2V$. The relationships between this and interaction energies of other dimers in $c(4 \times 2)$ and $p(2 \times 2)$ structures are $-2V + 2H - 4D(\text{in } c(4 \times 2)) < -2V(\text{at boundary}) < -2V - 2H + 4D(\text{in } p(2 \times 2))$. Therefore, considering the long-range interaction, it is reasonable for two type-P defects on neighboring rows to interact to form a pair in order to reduce the area with complete $p(2 \times 2)$ arrangement (Fig. 3(c)$\rightarrow$3(b)).

There exist another type of a pair of type-P defects as shown in Fig. 3(d), in which four dimers of the two type-P defects are buckled in the same direction. In this case, the interaction energy of the unit is low as $-4V + 2G - 2H + 2D$, however, a dimer row with complete $p(2 \times 2)$ arrangement is formed as shown in Fig. 3(d). Therefore, considering the long range interaction, this type would

not be formed. In fact, this structure was not observed at $80\,\mathrm{K}$.

Since E_{int} of a dimer at a boundary between the $c(4 \times 2)$ and $p(2 \times 2)$ arrangements is still higher than that of the $c(4 \times 2)$ structure, a pair of type-P defects is expected to move in order to reduce the area of the boundary. However, some type-P defect pairs were observed to move in the opposite direction; i.e., towards the upper side in Fig. 3(b), in a similar way to P_1 and P_2 in Fig. 1. The interaction energies of the upper and lower dimers in the type-P defect unit shown in Fig. 3(b), are $-V + G + 2H - 2D$ and $-V + G + 2D$, respectively. The difference between them is very slight, but the lower dimer is still less stable than the upper one, which also results in movement of type-P defect pairs towards the lower side in Fig. 3(b), similarly as expected from the energy of long-range ordering. Therefore, the observed movements may indicate that a dimer row with complete $p(2 \times 2)$ arrangement, as shown in Fig. 3(a), is very unstable, whereas a dimer row on a boundary between the $c(4 \times 2)$ and $p(2 \times 2)$ arrangements, as shown in Fig. 3(b), is stable at $80\,\mathrm{K}$. This result agrees well with the previous observations that a complete $p(2 \times 2)$ domain induced by a type-C defect was very unstable and led to the formation of apparently symmetric dimers, whereas a stable $p(2 \times 2)$ structure was formed at the boundaries of $c(4 \times 2)$ domains.[3-5, 9]

Even if type-P defects on dimer rows at the boundaries between areas with $c(4 \times 2)$ and $p(2 \times 2)$ structures (Fig. 3(e)) move along dimer rows, the total area with $p(2 \times 2)$ arrangement, indicated by rectangles with dots in Fig. 3(e), does not change. In addition, both the upper and lower dimers in the unit in Fig. 3(d) have an interaction energy E_{int} of $-V + G$. Therefore, a type-P defect on a boundary can move in both directions with the same probability. Once a type-P defect is introduced, for example from a step edge, it can fluctuate on the surface and form another boundary, as shown in Fig. 3(e). This may be the mechanism for the introduction of type-P defects to the surface.

Figures 4(a) and 4(b) show magnifications of the areas indicated by two $\triangledown$ in Figs. 2(a) and 2(b), and their schematic structures are drawn in Figs. 4(c) and 4(d), respectively. Gray rectangles in Figs. 4(c) and 4(d) indicate the areas with dimers ordered in $p(2 \times 2)$ arrangement. The $p(2 \times 2)$ domains change their positions with fluctuation of the type-P defects at their domain boundaries, however, total area seems to change little as expected.

Let us see an example of the observed surface changes more in detail. As is shown in Fig. 4(a), there exists a type-C′ defect as indicated by C′; three adjacent dimers are buckled in the same direction.[12] However, during the scan of one minute, the type-C′ defect was dissociated into the structure consisting of two type-P defects, one of which moved towards left, and the other remained at the same position as indicated by an arrow and C in Fig. 4(d). Therefore, a type-C′ defect is considered to be a compound defect which is formed by a type-C and a type-P defects. Anyway, if only the type-P defect have moved towards left, eight dimers which changed their
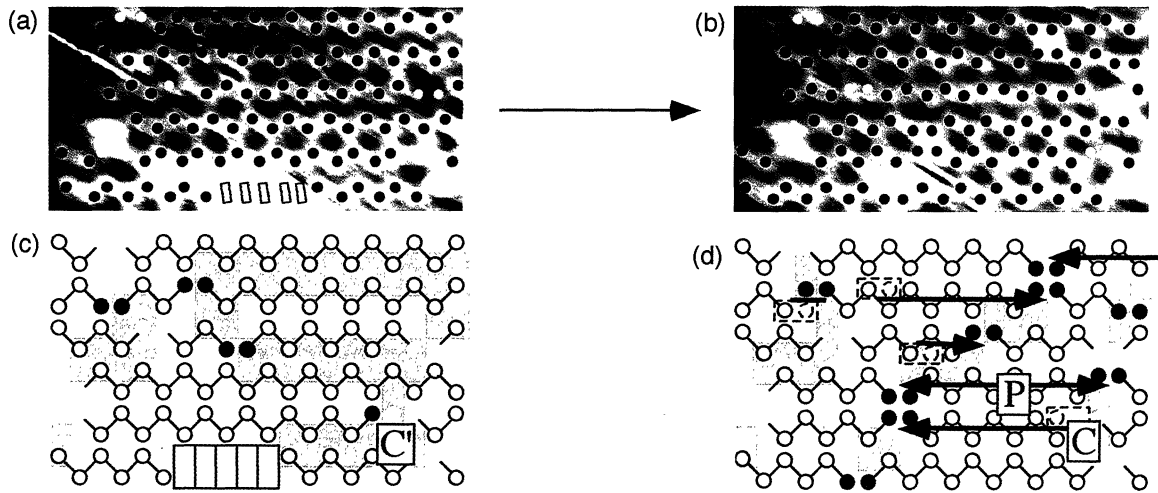
Fig. 4.   Magnifications ((a), (b)) and schematics ((c), (d)) of the areas indicated by two $\triangledown$ in Figs. 2(a) and 2(b), respectively. Only the upper Si atoms of the buckled dimers are illustrated using circles. Lines between the circles are drawn in order to compare the phase shift, and areas with $p(2 \times 2)$ arrangement are indicated by gray rectangles. Arrows in (b) indicate how type-P defects have moved from (a). Positions of type-P defects in (a) is overlapped in (b) with dashed rectangles.

buckling angles would have formed $p(2 \times 2)$ arrangement with the upper adjacent dimer row. In the case, the adjacent dimer row had formed complete $p(2 \times 2)$ arrangement with respect to its two adjacent dimer rows. However, since a dimer row with complete $p(2 \times 2)$ arrangement is very unstable as described above, it is not expected. In fact, complete $p(2 \times 2)$ arrangement is not formed there as shown in Fig. 4(d). With comparison of the structures in Figs. 4(c) and 4(d), it is clear that a pair of type-P defects was created during the scan of one minute on the adjacent dimer row as indicated by arrow P in Fig. 4(d). One of the type-P defect of the created pair moved towards left and formed a new pair with the type-P defect which moved from C, resulting in the reduction of the area with complete $p(2 \times 2)$ arrangement as expected. Total surface structural change can be understood with similar analysis for the all type-P defects on the surface. Formation of atom pairs during homoepitaxial growth of Si at 160 K observed by Wolkow may be related to the similar mechanism explained here.[13]

In conclusion, at 80 K, contrary to the phenomena previously obtained at 6 K, the $p(2 \times 2)$ arrangement is unstable, and two type-P defects on neighboring dimer rows interact to form a pair, thus reducing the area with $p(2 \times 2)$ arrangement. Since the temperature dependence of the observed phenomena is remarkable, the strength of the interaction between dimers may depend on the temperature more strongly than expected; for example, changes in the buckling angle and the charge density of the dimers may influence the coupling constants. Theoretical energy difference of ~ 1 meV between the $c(4 \times 2)$ and $p(2 \times 2)$ structures was obtained assuming zero temperature,[6] which may need to be compared with the previously observed phenomena at 6 K.[11] If the sign of the (2H-4D) changes from minus to plus at low temperature, the most stable structure changes from $c(4 \times 2)$ to

$p(2 \times 2)$ arrangement. Anyway, in order to understand the mechanism of dimer flip-flop motion and the stability of the surface structure, more detailed theoretical calculations taking into account the effects of the temperature dependence are necessary.

1) R. J. Hamers, R. M. Tromp and J. E. Demuth: Phys. Rev. B 34 (1986) 5343.
2) T. Tabata, T. Aruga and Y. Murata: Surf. Sci. 179 (1987) L63.
3) D. Badt, H. Wengelnik and H. Neddermeyer: J. Vac. Sci. & Technol. B 12 (1994) 2015.
4) A. R. Smith, F. K. Men, K.-J. Chao and C. K. Shih: J. Vac. Sci. & Technol. B 14 (1996) 914.
5) R. Wolkow: Phys. Rev. Lett. 68 (1992) 2636.
6) A. Ramstad, G. Brocks and P. J. Kelly: Phys. Rev. B 51 (1995) 14505.
7) A. Shkrebtii, R. D. Felice, M. Bertoni and R. Del Sole: Phys. Rev. B 51 (1995) 11201.
8) A. W. Munz, Ch. Ziegler and W. Gopel: Phys. Rev. Lett. 74 (1995) 2244.
9) H. Tochihara, T. Amakusa and M. Iwatsuki: Phys. Rev. B 50 (1994) 12262.
10) Y. Nakamura, H. Kawai and M. Nakayama: Phys. Rev. B 52 (1995) 8231.
11) H. Shigekawa, K. Miyake, M. Ishida, K. Hata, H. Oigawa, Y. Nannichi, A. Kawazu, R. Yoshizaki, T. Abe, T. Ozawa and T. Nagamura: J. Jpn. Appl. Phys. 35 (1996) L1081.
12) M. Uchikawa, M. Ishida, K. Miyake, K. Hata, R. Yoshizaki and H. Shigekawa: Surf. Sci. 357/358 (1996) 468.
13) R. Wolkow: Phys. Rev. Lett. 74 (1995) 4448.